Hindawi
Journal of Applied Mathematics
Volume 2023, Article ID 8570311, 15 pages
https://doi.org/10.1155/2023/8570311

Research Article

Mathematical Model and Analysis on the Impacts of Vaccination and Treatment in the Control of the COVID-19 Pandemic with Optimal Control

Alemzewde Ayalew,[1] **Yezbalem Molla**,[1] **Tenaw Tilahun**,[2] **and Tadele Tesfa**[1]

[1]*Department of Mathematics, Hawassa University, P.O. Box 05, Hawassa, Ethiopia*
[2]*Department of Mathematics, Mizan-Tepi University, Ethiopia*

Correspondence should be addressed to Alemzewde Ayalew; alemzewde@mtu.edu.et

Received 1 August 2022; Revised 23 November 2022; Accepted 19 January 2023; Published 3 March 2023

Academic Editor: Anum Shafiq

In this study, a nonlinear deterministic mathematical model that evaluates two important therapeutic measures of the COVID-19 pandemic: vaccination of susceptible and treatment for infected people who are in quarantine, is formulated and rigorously analyzed. Some of the fundamental properties of the model system including existence and uniqueness, positivity, and invariant region of solutions are proved under a certain meaningful set. The model exhibits two equilibrium points: disease-free and endemic equilibrium points under certain conditions. The basic reproduction number, R_0, is derived via the next-generation matrix approach, and the dynamical behavior of the model is explored in detail. The analytical analysis reveals that the disease-free equilibrium solution is locally as well as globally asymptotically stable when the associated basic reproduction number is less than unity which indicates that COVID-19 dies out in the population. Also, the endemic equilibrium point is globally asymptotically stable whenever the associated basic reproduction number exceeds a unity which implies that COVID-19 establishes itself in the population. The sensitivity analysis of the basic reproduction number is computed to identify the most dominant parameters for the spreading out as well as control of infection and should be targeted by intervention strategies. Furthermore, we extended the considered model to optimal control problem system by introducing two time-dependent variables that represent the educational campaign to susceptibles and continuous treatment for quarantined individuals. Finally, some numerical results are illustrated to supplement the analytical results of the model using MATLAB ode45.

1. Introduction

Nowadays, the world is faced with a number of issues, including climatic change, racism, terrorism, unemployment, poverty, and public health crises. Among them, the global coronavirus disease 2019 (COVID-19) outbreak is still a major public health concern. Severe acute respiratory syndrome-2 (SARS-CoV-2) is the virus that causes COVID-19 [1–4]. The first case of this new coronavirus, which frequently manifests as pneumonia, was found in Wuhan, China, in December 2019 [3, 5–7]. One of the things which make this disease so dangerous is that it spreads very quickly between people. Direct contact with contaminated surfaces and inhalation of respiratory droplets from infected individuals are the two ways that COVID-19 spreads from person to person [3, 6, 8, 9]. COVID-19 typically takes 2 to 14 days to incubate after being exposed to the virus [3, 10–12]. Fever, a dry cough, shortness of breath, and fatigue are some of the most prevalent clinical signs of COVID-19 [5, 13].

The outbreak was classified as a Public Health Emergency of International Concern by the World Health Organization (WHO) in January 2020 and as a pandemic on March 11, 2020 [14, 15]. More than 2.58 million fatalities and over 116.17 million confirmed cases were recorded as of March 7th, 2021 [16]. Globally, there have been more

than 197 million new cases, and of these, more than 4 million people have died until the end of July 2021 [17, 18]. The WHO report of COVID-19 indicated that on 10 August 2021, more than 202.14 million people were infected with the virus, and over 4.28 million have died.

The development of applicable intervention strategies to mitigate the COVID-19 outbreak requires a deep understanding of its transmission process and prevention programs. Mathematical modeling in epidemiology has become an effective tool for understanding and describing the dynamics of infectious disease [19]. The basic and important research subjects for epidemiological models are the existence of the threshold value which distinguishes whether the infectious disease will die out or persist via the local and global stability of the disease-free and endemic equilibrium [20].

Since the COVID-19 outbreak, different scholars have studied the transmission dynamics of the disease by considering different scenarios using mathematical modeling [1–3, 7, 10, 18, 21–40]. To the best of our knowledge, mathematical models that take the possibility of using additional preventative measures in addition to vaccination to stop the spread of COVID-19 are extremely uncommon. As a result, in this study, we are motivated to develop a model for COVID-19 transmission using model [41] as our framework by taking vaccination to susceptible human class and Holling type II with optimal control into consideration. In order to achieve this, we present SVIDR and this proposed model differs from others in that those susceptible people who received vaccinations joined the class of vaccinated humans, whereas other susceptible people who did not receive vaccinations might contract an infection from an infectious agent with the term $\beta SI/(\sigma + \eta I)$ and advance into the infectious class. The rest of this study is organized as follows. We formulated the transmission dynamics of the COVID-19 model in Section 2. The formulated model is analyzed in Section 3. The optimal control problem with some basic properties are discussed in Section 4. We illustrated numerical simulations of the model in Section 5. Finally, conclusion and conclusion remarks along with study suggestions are provided in Section 6.

2. Mathematical Model Formulation

In this section, we divided the entire population into five compartments based on the disease status of each individual: susceptible individuals (S), vaccinated individuals (V), individuals infected with COVID-19 (I), quarantined individuals (D), and recovered individuals (R). In the formulation of our model, the following assumptions are taken into account:

(i) When susceptible individuals receive the COVID-19 vaccination, they will join a class of humans who have received the vaccine at a rate of ϕ

(ii) The class of susceptible people only contract COVID-19 infection when they come into contact with an infected person at a rate of β

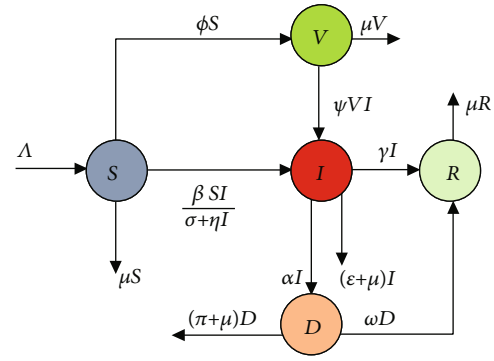

Figure 1: The schematic flowchart of COVID-19 dynamics.

(iii) The class of vaccine recipients can contract COVID-19 infection only when they come into contact with those who have the disease at a rate of ψ

(iv) The class of COVID-19-infected individuals can join either the quarantine class with the rate of α or recovered class with the rate of γ

(v) In addition to vaccination, susceptible people take other precautions against COVID-19

(vi) All parameters involved in the model are nonnegative

Individuals were recruited into the susceptible class with the recruitment rate Λ. We assumed that all compartments would experience the same amount of natural death μ. Susceptible individuals decrease due to COVID-19 infection following effective contact with infected individuals at the rate β. The infectious and quarantined human classes decrease due to COVID-19-induced death with the rate of ϵ and π, respectively. With this in mind, the total number of human population at a given time t is given by $N(t) = S(t) + V(t) + I(t) + D(t) + R(t)$. With regard to the above considerations, the compartmental developed COVID-19 model schematic flowchart is shown in Figure 1 and model parameters are described in Table 1.

The above model assumptions and Figure 1 lead to the following autonomous system of nonlinear differential equations:

$$\left.\begin{aligned}
\dot{S}(t) &= \Lambda - \frac{\beta SI}{\sigma + \eta I} - \phi S - \mu S \\
\dot{V}(t) &= \phi S - (\mu + \psi I)V \\
\dot{I}(t) &= \frac{\beta SI}{\sigma + \eta I} + \psi VI - (\mu + \epsilon + \gamma)I - \alpha I \\
\dot{D}(t) &= \alpha I - (\mu + \pi + \omega)D \\
\dot{R}(t) &= \gamma I + \omega D - \mu \mathrm{R}
\end{aligned}\right\}, \tag{1}$$

Table 1: Description of model parameters.

Notation	Biological meaning
Λ	The recruitment rate of susceptible individuals
ϕ	The progression rate of susceptibles into vaccinated individual class
μ	The natural death rate of all individuals
β	The contact rate of susceptibles with infectious individuals
ψ	The contact rate of vaccinated individuals with infected individuals
ω	Recovery rate of quarantined individuals into recovered individuals
ϵ	Disease-induced death rate of infectious individuals
π	Disease-induced death rate of quarantined individuals
γ	Recovery rate of infected individuals into recovered individuals' class
σ	Half saturation constant
η	Positive constant

Table 2: Baseline values for model parameters of the model system.

Parameter	Nominal value	Reference	Elasticity index
Λ	4721.5	[31]	+1
β	0.0108	[31]	+0.847
ψ	0.01	Assumed	+0.153
ϕ	0.0043	Assumed	-0.0132
γ	0.1	[3]	-0.219
α	0.22	Assumed	-0.481
σ	5	[48]	-1
ϵ	0.0271	[31]	No
π	0.4	[49]	No
η	1	[48]	No
μ	0.11	[30]	No
ω	0.2	Assumed	No

with the initial conditions:

$$\left.\begin{aligned} S(0) &= S_0 > 0 \\ V(0) &= V_0 \geq 0 \\ I(0) &= I_0 \geq 0 \\ D(0) &= D_0 \geq 0 \\ R(0) &= R_0 \geq 0 \end{aligned}\right\}. \tag{2}$$

3. Mathematical Analysis of the Model

In this section, the fundamental properties of the model system (1) are investigated, including the existence and uniqueness of solutions, nonnegativity of solutions, invariant region, basic reproduction number, equilibria, and its stability analysis.

Lemma 1 (existence and uniqueness of model solutions). *The model system (1) with initial condition (2) admits the unique solution in* $C(\mathbb{R}^+, \mathbb{R}_+^5), \forall t \geq 0$.

Proof. The model system (1) can be written in the form of $\dot{x} = f(x)$, where

$$\dot{x} = \begin{bmatrix} \dot{S}(t) \\ \dot{V}(t) \\ \dot{I}(t) \\ \dot{D}(t) \\ \dot{R}(t) \end{bmatrix},$$

$$f(x) = \begin{bmatrix} \Lambda - \dfrac{\beta SI}{\sigma + \eta I} - \phi S - \mu S \\ \phi S - (\mu + \psi I)V \\ \dfrac{\beta SI}{\sigma + \eta I} + \psi VI - (\mu + \epsilon + \gamma)\mathrm{I} - \alpha I \\ \alpha I - (\mu + \pi + \omega)\mathrm{D} \\ \gamma I + \omega D - \mu R \end{bmatrix}. \tag{3}$$

All the right-hand side components of the function $f(x)$ in the system (3) are continuously differentiable almost everywhere in $C(\mathbb{R}^+, \mathbb{R}_+^5)$, which implies that $f(x)$ is a family of C^1 on $\mathbb{R}_+^5$ for all $t \geq 0$. Hence, by the Picard–Lindelöf theorem [42], the model system (1) admits a unique solution locally in $\mathbb{R}_+^5$ for all time $t \geq 0$. This completes the proof of the theorem. □

Theorem 2 (nonnegativity of model solutions). *The solution set* $\{S(t), V(t), I(t), D(t), R(t)\}$ *of the model system (1) with initial condition (2) in the closed region* $\Omega \subset \mathbb{R}_+^5$ *is nonnegative for all future time* $t \geq 0$.

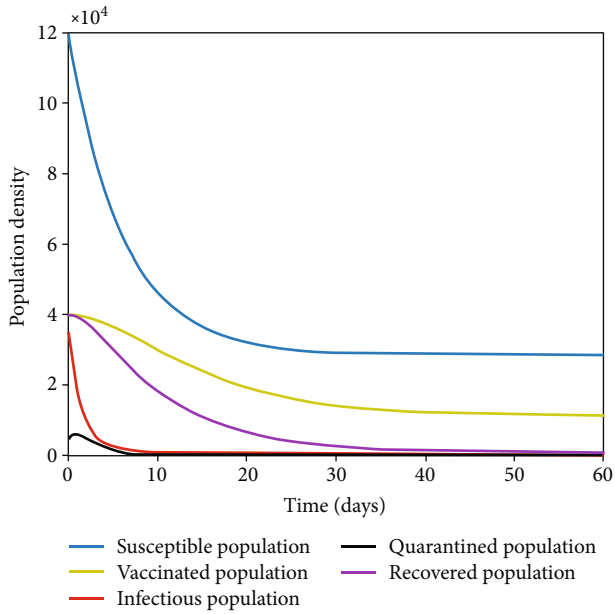

Figure 2: $R_0 = 0.0132 < 1$.

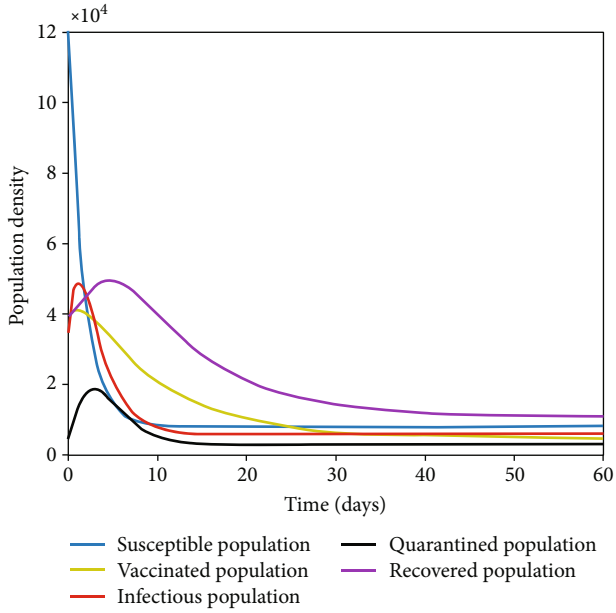

Figure 3: $R_0 = 1.1232 > 1$.

Proof. From the model system (1), we have that

$$\begin{aligned}
\dot{S}_{|S=0} &= \Lambda > 0,\\
\dot{V}_{|V=0} &= \phi S \geq 0, \quad \forall S \geq 0,\\
\dot{I}_{|I=0} &= \phi S \geq 0, \quad \forall S \geq 0,\\
\dot{D}_{|D=0} &= \alpha I \geq 0, \quad \forall I \geq 0,\\
\dot{R}_{|R=0} &= \gamma I + \omega D \geq 0, \quad \forall (I, D) \geq 0.
\end{aligned} \tag{4}$$

Hence, all the trajectories of model system (1) remain nonnegative for all nonnegative initial conditions. □

Theorem 3 (invariant region). *The closed region* $\Omega = \{(S, I, V, D, R) \in \mathbb{R}^5_+ : 0 \leq N(t) \leq \Lambda/\mu\}$ *is positively invariant and absorbing with respect to the set of nonlinear differential system of equations (1).*

Proof. Differentiating $N(t)$ with respect to time t and adding all the right-hand sides of model (1) together gives $\dot{N}(t) = \Lambda - \mu N - \epsilon I - \pi D$. Based on the non-negativity of model (1), we have that $N(t) = \Lambda - \mu N - \epsilon I - \pi D \leq \Lambda - \mu N$. Using Gronwall's inequality, the solution become: $N(t) \leq (\Lambda/\mu) + (N(0) - (\Lambda/\mu))e^{-ut}$. It follows that $N(t) \leq \Lambda/\mu$ as $t \longrightarrow \infty$. Hence, $\Omega = \{(S, I, V, D, R) \in \mathbb{R}^5_+ : 0 \leq N(t) \leq \Lambda/\mu\}$. Thus, the model is biologically meaningful and mathematically well-posed in the region Ω. □

3.1. Model Equilibria and Basic Reproduction Number

3.1.1. Disease-Free Equilibrium Point of the Model. To obtain the disease-free equilibrium (DFE), we equate the right-hand sides of model system (1) equal to zero at $I = D = 0$. Therefore, the disease-free equilibrium point of model system (1) is denoted by E_f and given by $E_f = (S^*, V^*, I^*, D^*, R^*) = (\Lambda/(\phi + \mu), \Lambda\phi/(\mu(\mu + \phi)), 0, 0, 0)$.

3.1.2. Basic Reproduction Number of the Model. In this subsection, we obtained the threshold parameter that governs the spread of a COVID-19 disease which is called the basic reproduction number, R_0. To obtain the basic reproduction number, we used the next-generation matrix method [43, 44] so that it is the spectral radius of the next-generation matrix. From model system (1), the rate that may cause new infections f and the rate of transfer v are

$$\begin{aligned}
f &= \begin{bmatrix} \dfrac{\beta SI}{\sigma + \eta I} + \psi VI \\ 0 \end{bmatrix},\\
v &= \begin{bmatrix} (\mu + \epsilon + \gamma)I + \alpha I \\ -\alpha I + (\mu + \pi + \omega)D \end{bmatrix},
\end{aligned} \tag{5}$$

respectively. The linearized matrix of f and v at the disease-free equilibrium point E_f is given by F and V as

$$\begin{aligned}
F &= \begin{bmatrix} \dfrac{\beta\Lambda}{\sigma(\phi + \mu)} + \dfrac{\phi\Lambda\psi}{\mu(\phi + \mu)} & 0 \\ 0 & 0 \end{bmatrix},\\
V &= \begin{bmatrix} (\mu + \epsilon + \gamma + \alpha) & 0 \\ -\alpha & (\omega + \mu + \pi) \end{bmatrix},
\end{aligned} \tag{6}$$

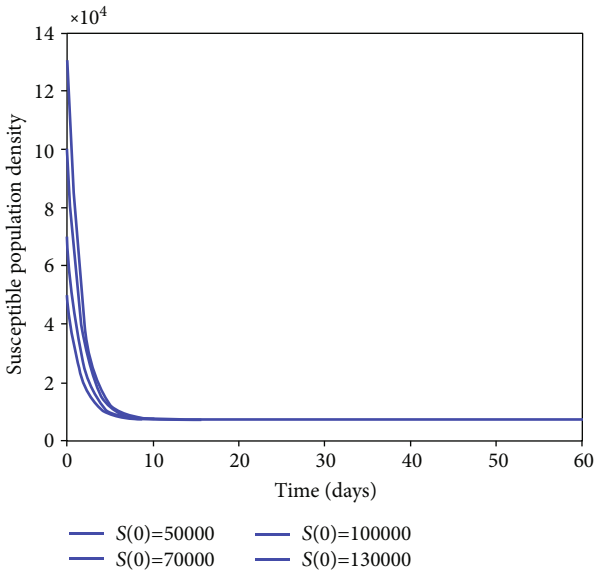

Figure 4: The time series plot of the susceptible population.

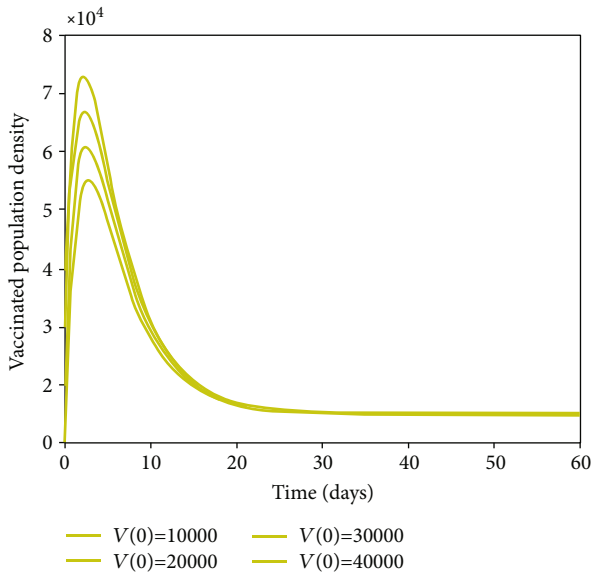

Figure 5: The time series plot of the vaccinated population.

respectively. Then, the inverse of V is obtained and given by

$$V^{-1} = \begin{bmatrix} \dfrac{1}{(\epsilon+\gamma+\mu+\alpha)} & 0 \\ \dfrac{\alpha}{(\pi+\omega+\mu)(\alpha+\gamma+\mu+\epsilon)} & \dfrac{1}{(\pi+\omega+\mu)} \end{bmatrix}. \tag{7}$$

Finally,

$$FV^{-1} = \begin{bmatrix} \dfrac{\Lambda(\beta\mu+\phi\sigma\psi)}{\mu(\phi+\mu)(\alpha+\mu+\gamma+\epsilon)} & 0 \\ 0 & 0 \end{bmatrix}. \tag{8}$$

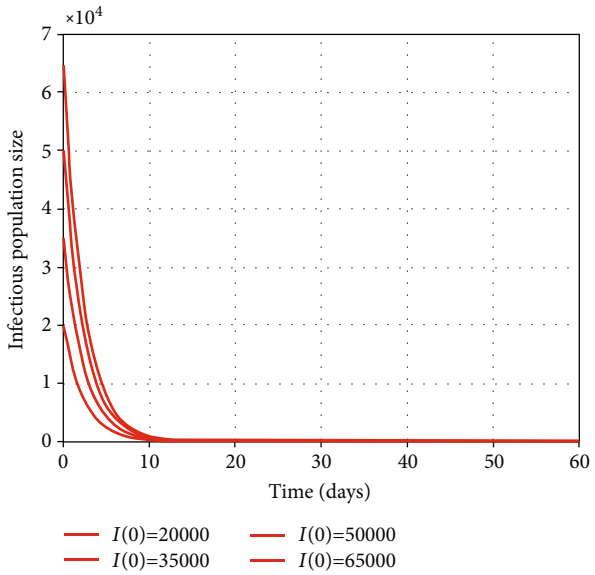

Figure 6: The time series plot of the infectious population.

The two eigenvalues of FV^{-1} are

$$\begin{aligned} \lambda_1 &= 0, \\ \lambda_2 &= \frac{\Lambda(\beta\mu+\phi\sigma\psi)}{\sigma\mu(\phi+\mu)(\alpha+\mu+\gamma+\epsilon)}. \end{aligned} \tag{9}$$

Indeed, the spectral radius of FV^{-1} is

$$\rho\left(FV^{-1}\right) = R_0 = \max\{\lambda_1, \lambda_2\} = \frac{\Lambda(\beta\mu+\phi\sigma\psi)}{\sigma\mu(\phi+\mu)(\alpha+\mu+\gamma+\epsilon)}. \tag{10}$$

From (10), $1/(\phi+\mu)$ and $1/(\alpha+\mu+\gamma+\epsilon)$ represent the time spent by susceptible and infectious individuals in states S and I, respectively.

3.2. Endemic Equilibrium Point of the Model. Besides the disease-free equilibrium point, the endemic equilibrium point is a positive steady-state solution where the disease persists in the population and it is calculated by setting all differential equations in model (1) equal to zero. Solving the first, second, fourth, and fifth equations in the system (1) gives as

$$\begin{aligned} S^{**} &= \frac{\Lambda(\sigma+\eta I^*)}{\beta I^* + k_1(\sigma+\eta I^*)}, \\ V^{**} &= \frac{\phi\Lambda}{(\mu+\psi I^*)(\beta I^* + k_1(\sigma+\eta I^*))}, \\ I^{**} &= \frac{\alpha I^*}{k_3}, \\ R^{**} &= \frac{(\gamma k_3 + \alpha\omega) I^*}{\mu k_3}, \end{aligned} \tag{11}$$

Then, substituting S^{**} and V^{**} into $\dot{I}$, we obtained the

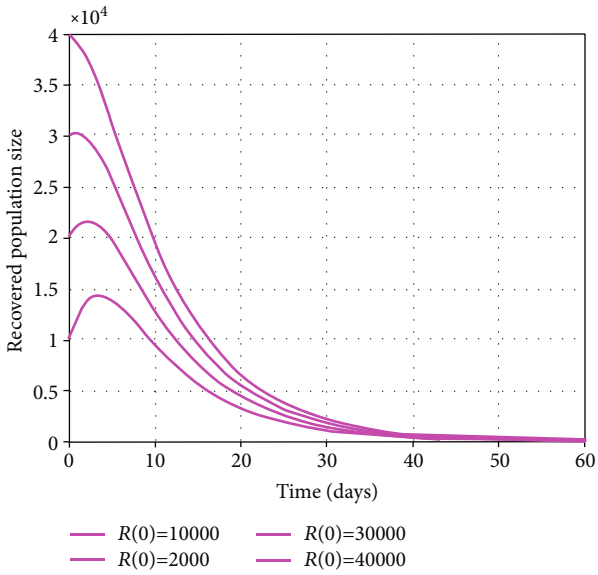

Figure 7: The time series plot of the recovered population.

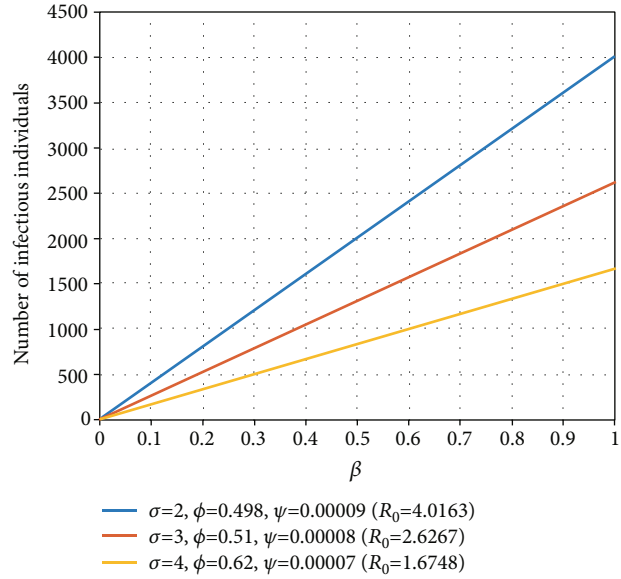

Figure 8: The effect of σ, ϕ, and ψ on R_0 in the presence of β.

quadratic equation and I^{**} is the positive solution calculated from

$$A(I^{**})^2 + BI^{**} + C = 0, \tag{12}$$

where

$$\begin{aligned} k_1 &= (\phi + \mu), \\ k_2 &= (\alpha + \gamma + \epsilon + \mu), \\ k_3 &= (\pi + \omega + \mu), \\ A &= k_2(\beta\psi + k_1\psi\eta), \\ B &= k_2(\beta\mu + \mu k_1\eta + k_1\psi\sigma) - \left(\beta\Lambda\psi + \phi(\psi)^2\Lambda\right), \\ C &= -\mu k_1 k_2\sigma(R_0 - 1). \end{aligned} \tag{13}$$

It follows that $C < 0$ whenever $R_0 > 1$ and the endemic equilibrium exist. Hence, the following result is established.

Proposition 4. *The positive endemic equilibrium point $E_p = (S^{**}, V^{**}, I^{**}, D^{**}, R^{**})$ of model system (1) exists when $R_0 > 1$.*

3.3. Stability Analysis of Model Equilibria. The subsequent theorems discuss the local and global stability analysis of disease-free (E_f) and disease-persistent equilibrium (E_p) points of model system (1).

Theorem 5. *The disease-free equilibrium point $E_f = (S^*, V^*, I^*, D^*, R^*)$ of model system (1) is locally asymptotically stable whenever $R_0 < 1$ and unstable whenever $R_0 > 1$.*

Proof. The linearized matrix of the system (3) at the disease-free equilibrium E_f is given by

$$L(E_f) = \begin{bmatrix} -k_1 & 0 & \dfrac{-\beta\Lambda}{\sigma k_1} & 0 & 0 \\ \phi & -\mu & \dfrac{-\psi\phi\Lambda}{\mu k_1} & 0 & 0 \\ 0 & 0 & \dfrac{\Lambda(\beta\mu + \phi\sigma\psi)}{\sigma\mu k_1} - k_2 & 0 & 0 \\ 0 & 0 & \alpha & -k_3 & 0 \\ 0 & 0 & \gamma & \omega & -\mu \end{bmatrix}, \tag{14}$$

where $k_1 = (\phi + \mu)$, $k_2 = (\mu + \epsilon + \alpha + \gamma)$, and $k_3 = (\mu + \pi + \omega)$ and the characteristic polynomial of $L(E_f)$ is expressed by

$$P(\lambda) = (\lambda + k_1)(\lambda + \mu)^2(\lambda + k_3)\left(\lambda - \left(\frac{\Lambda(\beta\mu + \phi\sigma\psi)}{\sigma\mu k_1} - k_2\right)\right) = 0. \tag{15}$$

The five eigenvalues of (15) are

$$\begin{aligned} \lambda_1 &= -k_1 = -(\phi + \mu) < 0, \\ \lambda_2 &= \lambda_3 = -\mu < 0, \\ \lambda_4 &= -k_3 = -(\alpha + \gamma + \mu + \epsilon) < 0, \\ \lambda_5 &= \frac{\Lambda(\beta\mu + \phi\sigma\psi)}{\sigma\mu k_1} - k_2 = \frac{\Lambda(\beta\mu + \phi\sigma\psi)}{\sigma\mu(\mu + \phi)} \\ &\quad - (\mu + \gamma + \epsilon + \alpha) = (\mu + \gamma + \epsilon + \alpha)\left(\frac{\Lambda(\beta\mu + \phi\sigma\psi)}{\sigma\mu(\phi + \mu)(\mu + \gamma + \epsilon + \alpha)} - 1\right) \\ &= (\mu + \gamma + \epsilon + \alpha)(R_0 - 1). \end{aligned} \tag{16}$$

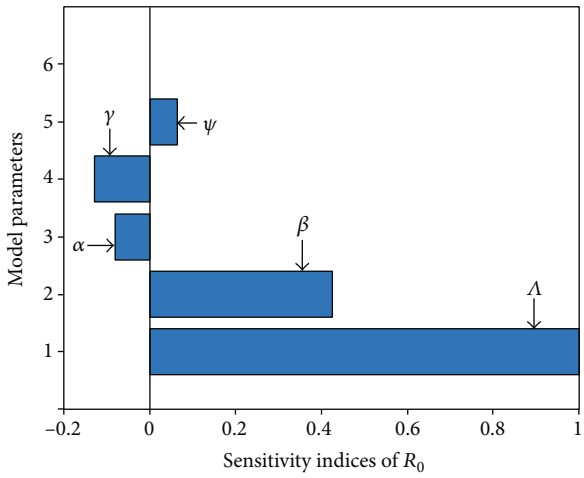

Figure 9: The numerical result of sensitivity analysis.

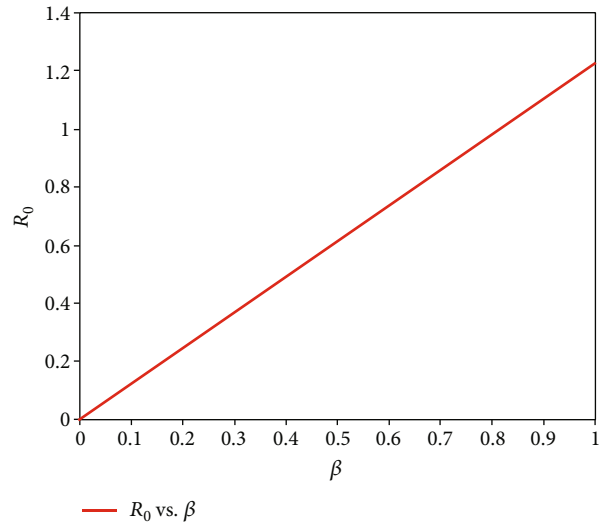

Figure 10: The effect of β on R_0.

It is obvious that $\lambda_1 < 0, \lambda_2 < 0, \lambda_3 < 0$, and $\lambda_4 < 0$, but $\lambda_5 = (\mu + \gamma + \epsilon + \alpha)(R_0 - 1) < 0$ provided that $(R_0 - 1) < 0$, which leads to $R_0 < 1$. Thus, the disease-free equilibrium point E_f of the system (1) is locally asymptotically stable for $R_0 < 1$. In epidemiological point of view, this result implies that COVID-19 cannot invade the community for $R_0 < 1$. Whenever $R_0 > 1$, the value of $\lambda_5 > 0$, which implies that there is one eigenvalue with positive real root and the disease-free equilibrium point E_f is unstable, and this indicates that COVID-19 invasion will occur within the society. □

Theorem 6. *The disease-free equilibrium point $E_f = (S^*, V^*, I^*, D^*, R^*)$ of model system (1) is globally asymptotically stable whenever $R_0 < 1$, otherwise unstable.*

Proof. To show the above result, we follow Castillo-Chavez et al.'s theorem [45]. The model system (1) can be written as

$$\begin{aligned} \dot{X} &= \mathscr{H}(X, Z) \\ \dot{Z} &= \mathscr{M}(X, Z), \quad \mathscr{M}(X, 0) = 0, \end{aligned} \tag{17}$$

where $X = (S, V, R) \in R^3$ denotes the non-infectious human populations, while $Z = (I, D) \in R^2$ denotes the infectious human populations. According to Castillo-Chavez et al.'s theorem [45], to be the disease-free equilibrium point E_f of the model system (1) globally asymptotically stable, the following two necessary conditions (H_1) and (H_2) must be met:

(H_1) For $\dot{X} = \mathscr{H}(X^*, 0)$, X^* is globally asymptotically stable. Thus, in the system (1) at E_f, we have that $\lim_{t \longrightarrow \infty} (S(t), V(t), R(t)) = (\Lambda/(\mu + \phi), \phi\Lambda/(\mu(\phi + \mu)), 0)$. Hence, X^* is globally asymptotically stable.

$(H_2) \mathscr{M}(X, Z) = AZ - \widehat{\mathscr{M}}(X, Z)$, where $\widehat{\mathscr{M}}(X, Z) \geq 0$ in the closed region Ω.

Now, consider $\mathscr{M}(X, Z) = AZ - \widehat{\mathscr{M}}(X, Z) \Rightarrow \widehat{\mathscr{M}}(X, Z) = AZ - \mathscr{M}(X, Z)$.

$$\widehat{\mathscr{M}}(X, Z) = \begin{bmatrix} \dfrac{\partial I(E_f)}{\partial I} & \dfrac{\partial I(E_f)}{\partial D} \\ \dfrac{\partial D(E_f)}{\partial I} & \dfrac{\partial D(E_f)}{\partial D} \end{bmatrix} \begin{bmatrix} I \\ D \end{bmatrix} - \begin{bmatrix} \dfrac{dI}{dt} \\ \dfrac{dD}{dt} \end{bmatrix},$$

$$\widehat{\mathscr{M}} = \begin{bmatrix} \dfrac{\beta\Lambda\mu + \psi\sigma\phi\Lambda}{\sigma\mu(\phi + \mu)} - (\mu + \epsilon + \alpha + \gamma) & 0 \\ \alpha & -(\mu + \pi + \omega) \end{bmatrix}$$

$$\begin{bmatrix} I \\ D \end{bmatrix} - \begin{bmatrix} \dfrac{\beta SI}{\sigma + \eta I} + \psi VI - (\mu + \epsilon + \gamma + \alpha)I \\ \alpha I - (\mu + \pi + \omega)D \end{bmatrix}. \tag{18}$$

From $\widehat{\mathscr{M}}$, A is a Metzler matrix (off diagonal elements of A are nonnegative in the closed region Ω in which the model gives biological sense).

Further simplification on $\widehat{\mathscr{M}}(X, Z)$, we get that

$$\widehat{\mathscr{M}} = \begin{bmatrix} \dfrac{(\beta\mu + \phi\sigma\psi)\Lambda I}{\sigma\mu(\phi + \mu)} - \left(\dfrac{\beta S}{\sigma + \eta I} + \psi V\right) I \\ 0 \end{bmatrix} \geq 0, \tag{19}$$

since at disease-free equilibrium point E_f, the solutions of the first and the second equation in system (1) become $S(t) = (\Lambda/(\phi + \mu)) + (S(0) - (\Lambda/(\phi + \mu)))e^{-(\phi+\mu)t} \leq \Lambda/(\phi + \mu)$ and $V(t) = (\Lambda\phi/(\mu(\phi + \mu))) + (1/\mu)(S(0) - (\Lambda/(\phi + \mu)))e^{-(\phi+\mu)t} \leq \Lambda\phi/(\mu(\phi + \mu))$ as $t \longrightarrow \infty$. This implies that condition (H_2) is fulfilled.

As a result, the disease-free equilibrium point E_f is globally asymptotically stable. □

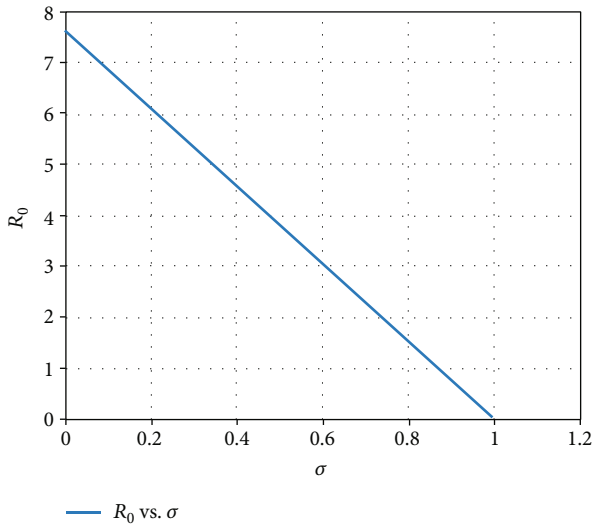

Figure 11: The effect of σ on R_0.

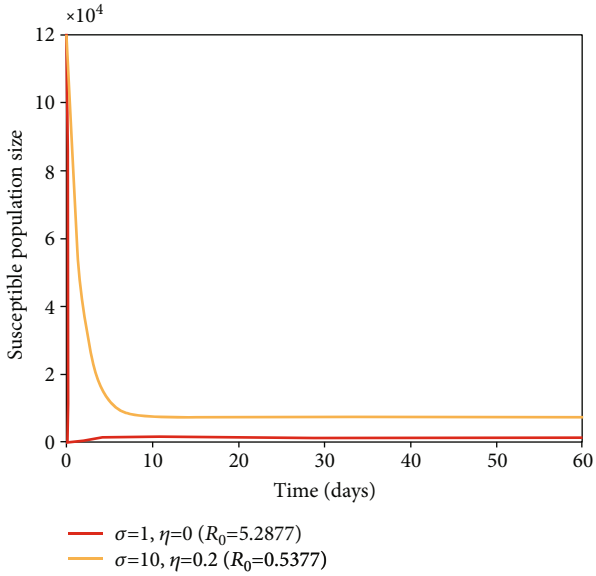

Figure 12: The effect of σ and η on the number of susceptible population.

Theorem 7. *The positive endemic equilibrium point* $E_p = (S^{**}, V^{**}, I^{**}, D^{**}, R^{**})$ *of model (1) is globally asymptotically stable whenever* $R_0 > 1$.

Proof. To prove this theorem, we employ the Dulac criterion [46] by taking $\mathscr{L}(I, D) = 1/ID$ as the candidate of Dual's function for model system (1) and $\mathscr{F} = (S, V, I, D, R)$.

Since $\mathscr{L}(I, D) > 0, \forall I, D > 0$, we have that

$$L(S, V, I, D, R) = \frac{d\mathscr{L}\mathscr{F}}{dt} = \frac{dfS}{dt} + \frac{dfV}{dt} + \frac{dfI}{dt} + \frac{dfD}{dt} + \frac{dfR}{dt}$$

$$= \frac{\partial}{\partial S}\left(\frac{1}{ID}\left(\Lambda - \frac{\beta SI}{\sigma + \eta I} - k_1 S\right)\right)$$

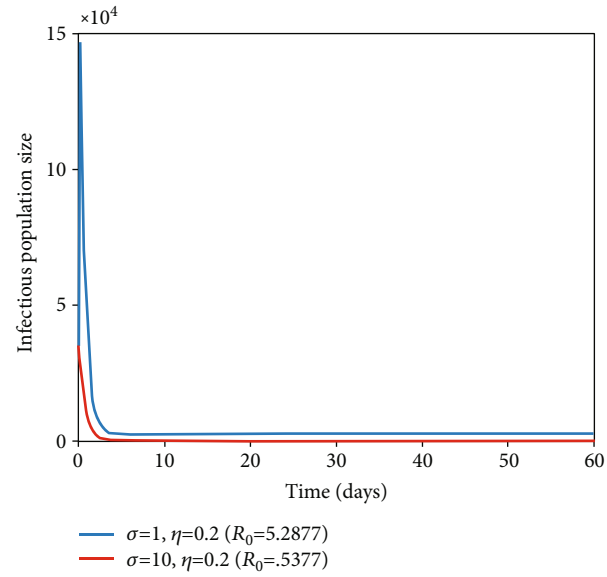

Figure 13: The effect of σ and η on the number of infectious population.

$$+ \frac{\partial}{\partial V}\left(\frac{1}{ID}(\phi S - (\mu + \psi I)V)\right)$$

$$+ \frac{\partial}{\partial I}\left(\frac{1}{ID}\left(\frac{\beta SI}{\sigma + \eta I} + \psi VI - k_2 I\right)\right)$$

$$+ \frac{\partial}{\partial D}\left(\frac{1}{ID}(\alpha I - k_3 D)\right)$$

$$+ \frac{\partial}{\partial R}\left(\frac{1}{ID}(\gamma I + \omega D - \mu R)\right)$$

$$= \frac{-\beta}{D(\sigma + \eta I)} - \frac{k_1}{ID} - \frac{(\mu + \psi I)}{ID}$$

$$- \frac{\alpha}{D^2} - \frac{\mu}{ID} - \frac{\beta \eta S}{(\sigma + \eta I)^2} < 0. \quad (20)$$

□

According to Dual's criterion [46], the model system (1) does not exhibit any periodic solution in the region Ω and, hence, the disease-persistent equilibrium point E_p is globally asysmptotically stable whenever $R_0 > 1$. This finding from an epidemiological perspective suggests that the number of infectious agents may fluctuate, making it challenging to allocate resources for disease control.

3.4. Sensitivity Analysis of Model Parameters. In this subsection, we investigate sensitivity analysis used to discover the most dominant parameters for the spreading out as well as control of infection in the society. To go through sensitivity analysis, we follow the classical approach used by Chitnis et al. [47].

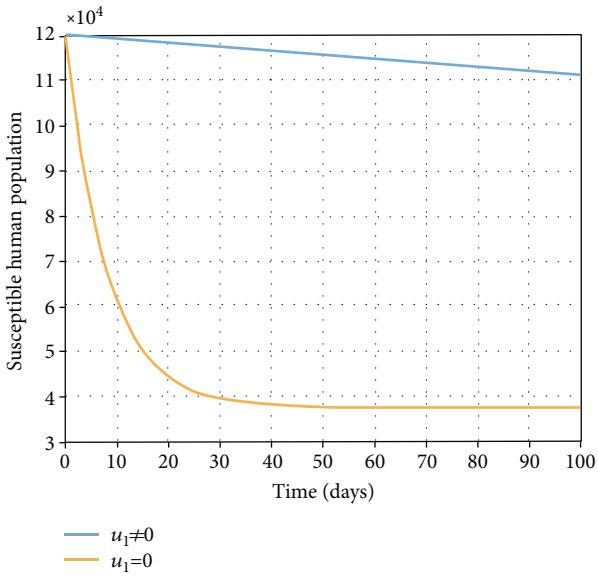

Figure 14: Susceptible individuals with and without prevention strategy u_1.

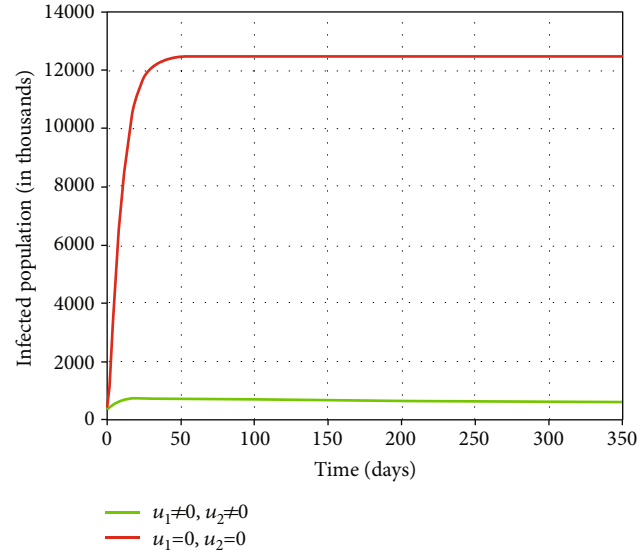

Figure 15: Infectious individuals with and without prevention strategy u_1 and intervention strategy u_2.

Definition 8. The normalized forward sensitivity index of variable R_0 that depends differentiability on an index parameter v is defined as $\mathcal{S}_v^{R_0} = (v/R_0).(dR_0/dv)$ [47].

Here, for example, $\mathcal{S}_v^{R_0} \cong +0.1$ means increasing (or decreasing) the value of v by 10%, which always results to increase (or decrease) the value of R_0 by 10%, whereas $\mathcal{S}_v^{R_0} = 0.1$ means increasing (or decreasing) the value of v by 10%, which always results to decrease (or increase) R_0 by 10%.

We assessed the sensitivity indices of the system (1) in a similar manner, and the results are as follows:

$$\begin{aligned}
\mathcal{S}_\beta^{R_0} &= 1,\\
\mathcal{S}_\beta^{R_0} &= \frac{\beta}{\beta\mu + \phi\sigma\psi},\\
\mathcal{S}_\phi^{R_0} &= \frac{\phi\mu(\delta\psi - \beta)}{(\phi+\mu)(\sigma\psi\phi + \mu\beta)},\\
\mathcal{S}_\alpha^{R_0} &= \frac{-\alpha}{(\alpha+\mu+\gamma+\varepsilon)},\\
\mathcal{S}_\phi^{R_0} &= \frac{\phi\mu(\delta\psi - \beta)}{(\phi+\mu)(\sigma\psi\phi + \mu\beta)},\\
\mathcal{S}_\delta^{R_0} &= \frac{-\beta\mu\sigma}{(\beta\mu + \phi\psi\sigma)},\\
\mathcal{S}_\psi^{R_0} &= \frac{\phi\mu\psi}{(\beta\mu + \phi\psi\sigma)}.
\end{aligned} \tag{21}$$

Numerical results of sensitivity analysis from baseline model parameters are arranged in a descending order from Table 2. However, in the study of sensitivity analysis, it is not biologically reasonable to increase or decrease human mortality rates to control disease outbreak, and hence we do not consider.

3.5. Interpretation of Sensitivity Indices. It is noted from Table 2 that the value of R_0 increases when the parameter values Λ, β, and ψ increase while other parameter values are kept fixed. This means the spread of COVID-19 increases due to the reason that the basic reproduction number increases as their values increase; it means that the average number of secondary cases of infection increases in the community while the rest of parameters kept fixed. In contrast, parameters σ, α, ϕ, and γ have a positive impact in the reduction of the burden of the disease in the community as their values increase while the others are kept constant. And also, as their values increase, the basic reproduction number decreases. This means the spread of the virus decreases since raising the values of these parameters will consequently decrease the number of total infected population.

4. Extension of the Model into Optimal Control

In this section, we consider the optimal control of model (1), which describes the interaction of educational campaign with susceptibles and pharmaceutical interventions of the infected individuals. The ultimate goal of optimal control is to minimize the total number of infected individuals with minimum cost. We perform optimal control to the system (1) to investigate the impact of implementing continuous educational awareness creation and pharmaceutical intervention to mitigate the COVID-19 outbreak. To proceed with this, we introduced a set of time-dependent control variables $u_1(t)$ and $u_2(t)$ where

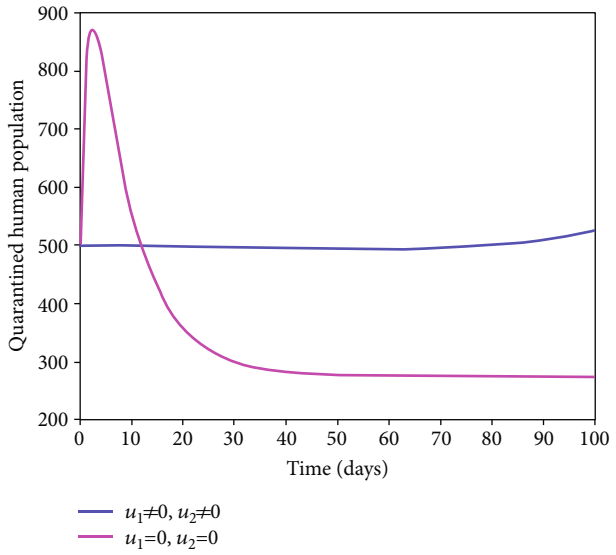

Figure 16: Quarantined individuals with and without prevention strategy u_1 and intervention strategy u_2.

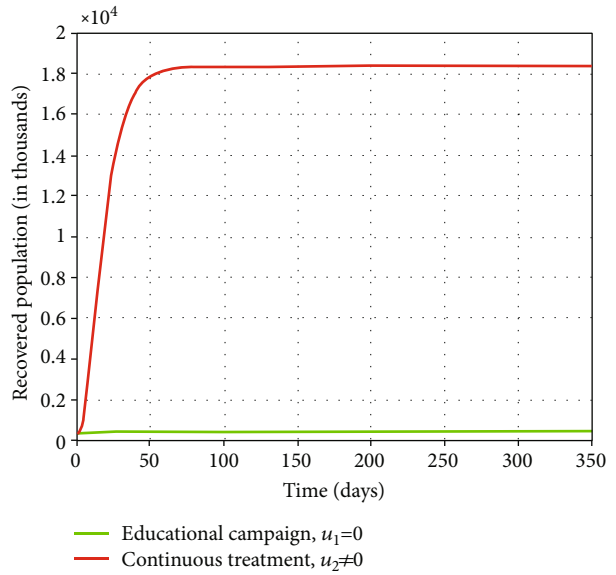

Figure 17: Recovered individuals with and without intervention strategy u_2.

(i) $u_1(t)$ denotes the efforts intended for susceptible individuals to create awareness through all media outlets

(ii) $u_2(t)$ denotes the efforts intended to encourage continuous treatment usually for quarantined individuals

For simplicity of notation, we represent $u_1(t) = u_1$ and $u_2(t) = u_2$. After incorporating the above intervention strategies in model (1), we get an optimal control model

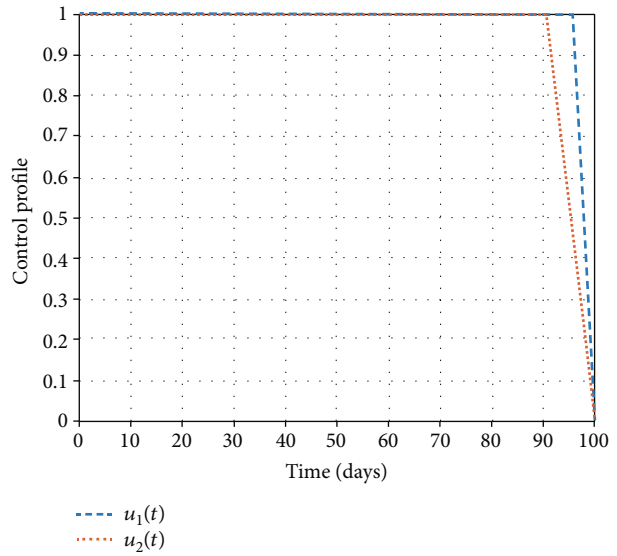

Figure 18: The profile of optimal controls u_1 and u_2.

described by

$$\begin{aligned}
\dot{S}(t) &= \Lambda - (1-u_1)\frac{\beta SI}{\sigma + \eta I} - \phi S - \mu S,\\
\dot{V}(t) &= \phi S - (\mu + \psi I)V,\\
\dot{I}(t) &= (1-u_1)\frac{\beta SI}{\sigma + \eta I} + \psi VI - (\mu + \epsilon + \gamma)I - \alpha I,\\
\dot{D}(t) &= \alpha I - (\mu + \pi + \omega + u_2)D,\\
\dot{R}(t) &= \gamma I + (\omega + u_2)D - \mu R.
\end{aligned} \tag{22}$$

The optimal control variables u_1 and u_2 minimize the objective function subject to system (23). The objective function is defined as

$$J(u_1, u_2) = \min_{u_1, u_2} \int_0^{t_f} \left[A_1 I(\tau) + A_2 D(\tau) + B_1 u_1^2(\tau) + B_2 u_2^2(\tau)\right] d\tau, \tag{23}$$

where t_f is fixed final time and the positive coefficients A_1, A_2, B_1, and B_2 are constants that balance the cost and the number of infected individuals at time t. In this paper, since the cost of the controls may not be measured linearly, we use the quadratic form as frequently used in [50, 51]. The ultimate goal is to find the optimal control (u_1^*, u_2^*) such that

$$J(u_1^*, u_2^*) = \min \{J(u_1, u_2) : u_1, u_2 \in U\}. \tag{24}$$

The controls u_1 and u_2 are assumed to be at least Lebesgue measurable on $[0, t_f]$ [52].

4.1. Existence of Optimal Control Problem

Theorem 9. *There exists an optimal control (u_1^*, u_2^*) that minimizes the objective function $J(u_1, u_2)$, subject to the control system (22).*

Proof. To show the existence of optimal control, we denote the right-hand sides of system (22) by $z(t, \vec{x}, \vec{u})$. Then, to prove the existence of optimal control, we follow the same procedure as [53, 54]. To achieve this result, the following conditions must be met:

(1) z is of class C^1, and there exists a constant c such that

$$|z(t,0,0)| \le c, \left|z_{\vec{x}}\left(t, \vec{x}, \vec{u}\right)\right| \le c\left(1 + \left|\vec{u}\right|\right), \left|z_{\vec{u}}\left(t, \vec{x}, \vec{u}\right)\right| \le c \tag{25}$$

(2) The admissible set of all solutions to system (22) with corresponding control in U_{ad} is nonempty

(3) There exist functions d_1 and d_2 such that $z(t, \vec{x}, \vec{u}) = d_1(t, \vec{x}) + d_2(t, \vec{x})\vec{u}$

(4) The control set $U = [0,1] \times [0,1]$ is closed, convex, and compact

(5) The integrand of the objective function is convex in U

To verify condition (1), rewrite

$$z\left(t, \vec{x}, \vec{u}\right) = \begin{bmatrix} \Lambda - (1-u_1)\dfrac{\beta SI}{\sigma + \eta I} - (\mu + \phi)S \\ \phi S - (\mu + \psi I)V \\ (1-u_1)\dfrac{\beta SI}{\sigma + \eta I} + \psi VI - (\psi + \epsilon + \gamma + \alpha)I \\ \alpha I - (u_2 + \pi + \mu + \omega)D \\ \gamma I + (\omega + u_2)D - \mu R \end{bmatrix}. \tag{26}$$

Then, one can see that $z(t, \vec{x}, \vec{u})$ is of class C^1 and $|z(t, 0, 0)| = \Lambda$.

Moreover, consider

$$\left|z_{\vec{x}}\left(t, \vec{x}, \vec{u}\right)\right| = \left|\begin{bmatrix} -(1-u_1)\dfrac{\beta I}{\sigma + \eta I} - (\mu + \phi) & 0 & -(1-u_1)\dfrac{\beta \sigma S}{(\sigma + \eta I)^2} & 0 & 0 \\ \phi & -(\mu + \psi I) & -\phi V & 0 & 0 \\ (1-u_1)\dfrac{\beta S}{(\sigma + \eta I)} & (1-u_1)\dfrac{\beta \sigma I}{(\sigma + \eta I)^2} + \psi V - k_1 & 0 & 0 & 0 \\ 0 & 0 & \alpha & -(u_2 + k_2) & 0 \\ 0 & 0 & \gamma & (\omega + u_2) & -\mu \end{bmatrix}\right|, \tag{27}$$

where $k_1 = (\alpha + \gamma + \psi + \epsilon)$, $k_2 = (\pi + \mu + \omega)$, and

$$\left|z_{\vec{u}}\left(t, \vec{x}, \vec{u}\right)\right| = \left|\begin{bmatrix} \dfrac{\beta SI}{(\sigma + \eta I)} & 0 \\ 0 & 0 \\ -\dfrac{\beta SI}{(\sigma + \eta I)} & 0 \\ 0 & -D \\ 0 & D \end{bmatrix}\right|. \tag{28}$$

Since S, V, I, D, and R are bounded, hence, there exists a constant c such that

$$|z(t,0,0)| \le c, \left|z_{\vec{x}}\left(t, \vec{x}, \vec{u}\right)\right| \le c\left(1 + \left|\vec{u}\right|\right), \left|z_{\vec{u}}\left(t, \vec{x}, \vec{u}\right)\right| \le c. \tag{29}$$

This shows that condition (1) is satisfied.

According to condition (1), a unique solution for the constant controls exist, which will improve that condition (2), is met.

Beside this,

$$z\left(t, \vec{x}, \vec{u}\right) = \begin{bmatrix} \Lambda - \dfrac{\beta SI}{\sigma + \eta I} - (\mu + \phi)S \\ \phi S - (\mu + \psi I)V \\ \dfrac{\beta SI}{\sigma + \eta I} + \psi VI - (\psi + \epsilon + \gamma + \alpha)I \\ \alpha I - (\pi + \mu + \omega)D \\ \gamma I + \omega D - \mu R \end{bmatrix} + \begin{bmatrix} \dfrac{\beta SI}{\sigma + \eta I} & 0 \\ -\dfrac{\beta SI}{\sigma + \eta I} & 0 \\ 0 & -D \\ 0 & D \end{bmatrix} \begin{bmatrix} u_1 \\ u_2 \end{bmatrix}. \tag{30}$$

This means condition (3) holds. The control set U is closed and bounded, hence compact. This verifies condition (10). Finally, we try to verify condition (15), (i.e., the convexity of the integrand of the objective function). We must ensure that for any two values $\vec{u}$ and $\vec{k}$ of the control vector

and a constant $m \in [0, 1]$, the following inequality holds:

$$(1-m)f\left(t, \vec{x}, \vec{u}\right) + mf\left(t, \vec{x}, \vec{k}\right) \geq f\left(t, \vec{x}, (1-m)\vec{u} + m\vec{k}\right), \tag{31}$$

where

$$f\left(t, \vec{x}, \vec{u}\right) = A_1 I + A_2 D + B_1 u_1^2 + B_2 u_2^2. \tag{32}$$

Furthermore,

$$\begin{aligned}(1-m)f\left(t, \vec{x}, \vec{u}\right) + mf\left(t, \vec{x}, \vec{k}\right) \\ = A_1 I + A_2 D + (1-m)\left(B_1 u_1^2 + B_2 u_2^2\right) + m\left(B_1 k_1^2 + B_2 k_2^2\right),\end{aligned} \tag{33}$$

and also,

$$\begin{aligned}f\left(t, \vec{x}, (1-m)\vec{u} + m\vec{k}\right) \\ = A_1 I + A_2 D + B_1[(1-m)u_1 + mk_1]^2 + B_2[(1-m)u_2 + mk_2]^2.\end{aligned} \tag{34}$$

Then,

$$\begin{aligned}(1-m)f\left(t, \vec{x}, \vec{u}\right) + mf\left(t, \vec{x}, \vec{k}\right) - f\left(t, \vec{x}, (1-\mathrm{m})\vec{u} + m\vec{k}\right) \\ = (1-m)\left(B_1 u^2{}_1 + B_2 u^2{}_2\right) + m\left(B_1 k^2{}_1 + B_2 k^2{}_2\right) \\ - B_1[(1-m)u_1 + mk_1]^2 + B_2[(1-m)u_2 + mk_2]^2 \\ = B_1\left[(1-m)u^2{}_1 + mk^2{}_1 - [(1-m)u_1 + mk_1]^2\right] \\ + B_2\left[(1-m)u^2{}_2 + mk^2{}_2 - [(1-m)u_2 + mk_2]^2\right] \\ = B_1\left[m(1-m)(u_1 - k_1)^2\right] + B_2\left[m(1-m)(u_2 - k_2)^2\right] \geq 0.\end{aligned} \tag{35}$$

This shows that condition (15) is fulfilled.

Hence, the proof of the theorem is completed. □

4.2. Characterization of the Optimal Control. Now, to solve the optimal control problem (23), we have constructed the Lagrangian equation as follows:

$$L(t, x, u) = \frac{dJ}{dt} = A_1 I(t) + A_2 D(t) + B_1 u_1^2(t) + B_2 u_2^2(t). \tag{36}$$

The necessary conditions that an optimal control should satisfy are derived from Pontryagin's Maximum Principle [33, 34].

To minimize the Lagrangian, we have constructed the Hamiltonian equation by

$$H(t, x, u, \xi) \quad = \frac{dJ}{dt} + \sum_{i=1}^{5} \xi_i f_i = L(t, x, u) + \sum_{i=1}^{5} \xi_i f_i, \tag{37}$$

where $L(t, x, u) = A_1 I + A_2 D + B_1 u_1^2(t) + B_2 u_2^2(t)$ and $f_i, i = 1, 2, 3, 4, 5$ are the right-hand side components of (22) and $\xi = (\xi_1, \xi_2, \xi_3, \xi_4, \xi_5) \in \mathbb{R}^5$ are costate variables associated to the state variables S, L, A, I, and R which can be determined from second partial derivatives of H with respect to state variables as follows:

$$\begin{aligned}\frac{d\xi_1}{dt} &= \frac{-\partial H}{\partial S}, \\ \frac{d\xi_2}{dt} &= \frac{-\partial H}{\partial V}, \\ \frac{d\xi_3}{dt} &= \frac{-\partial H}{\partial I}, \\ \frac{d\xi_4}{dt} &= \frac{-\partial H}{\partial D}, \\ \frac{d\xi_5}{dt} &= \frac{-\partial H}{\partial R}.\end{aligned} \tag{38}$$

It follows that

$$\begin{aligned}\dot{\xi}_1 &= \left[(1-u_1)\frac{\beta I}{\sigma + \eta I} + \alpha_1\right]\xi_1 - \phi\xi_2 - (1-u_1)\frac{\beta I \xi_3}{\sigma + \eta I}, \\ \dot{\xi}_2 &= (\mu + \psi I)\xi_2 - \psi I \xi_3, \\ \dot{\xi}_3 &= -A_1 + (1-u_1)\frac{\beta\delta\xi_1}{(\delta + \eta I)^2} + \psi V \xi_2 + \left[\alpha_2 - \psi V - (1-u_1)\frac{\beta\sigma S}{(\sigma + \eta I)^2}\right]\xi_3 - \alpha\xi_4 - \gamma\xi_5, \\ \dot{\xi}_4 &= A_2 + (\alpha_3 + u_2)\xi_4 - (\omega + u_2)\xi_5, \\ \dot{\xi}_5 &= \mu\xi_5,\end{aligned} \tag{39}$$

where $a_1 = (\phi + \mu)$, $a_2 = (\alpha + \mu + \gamma + \epsilon)$, and $a_3 = (\mu + \pi + \omega)$, with transversality conditions:

$$\xi_1(t_f) = \xi_2(t_f) = \xi_3(t_f) = \xi_4(t_f) = \xi_5(t_f) = 0. \tag{40}$$

Theorem 10. *The optimal control set $\{u_1^*(t), u_2^*(t)\}$ that minimizes $J(u_1, u_2)$ over the region U is obtained and presented in compact form as*

$$\begin{cases} u_{1(t)} = \min\{1, \max(0, u_\Delta)\}, \\ u_{2(t)} = \min\{1, \max(0, u_\nabla)\}, \end{cases} \tag{41}$$

where

$$\begin{aligned}u_\Delta &= \frac{\beta S I(\xi_3 - \xi_1)}{2B_1(\sigma + \eta I)}, \\ u_\nabla &= \frac{D(\xi_4 - \xi_5)}{2B_2}.\end{aligned} \tag{42}$$

Proof. The proof is similar to [55]. □

5. Numerical Results and Discussion

In this section, we carried out some numerical results of the model to verify the theoretical results by using MATLAB ode45 solver with the following initial conditions: $S(0) =$

120,000, $V(0) = 40{,}000$, $I(0) = 35{,}000$, $D(0) = 5000$, and $R(0) = 40,000$. Here, it is important to note that the initial conditions and parameter values used for simulation purpose are taken from the previous published articles and some others are assumed.

Figure 2 shows that all trajectories converge to their disease-free equilibrium point component when $\psi = 0.0000007$, $\phi = 0.043$, $\varepsilon = 0.271$, and other parameters values are from Table 1. This result supported the analytical conclusion that the disease-free equilibrium point is stable for $R_0 < 1$ stated from Theorem 5 and the outbreak of COVID-19 may reduce within the society. Figure 3 illustrates that all solution curves approach to their endemic equilibrium point component when parameter values are $\beta = 0.408$, $\alpha = 0.32$, $\pi = 0.34$, $\phi = 0.063$, $\sigma = 2$, and $\varepsilon = 0.0271$ and other parameter values are taken from Table 2 . This result confirmed with the theoretical result that the COVID-19 persistent equilibrium point is globally asymptotically stable for $R_0 = 1.1232 > 1$ stated in Theorem 6 and reinvasion of the COVID-19 outbreak occurs within the population.

Figures 4–7 show a time-serious plot of the total number of susceptible, immunized, infectious, and recovered human populations, with varying initial values, at the disease-free equilibrium point, where the basic reproduction number is less than unity. From Figure 8, it can be seen that large value of σ or ϕ and small value of ψ in the presence of β can lead to a small value of R_0. That is to say, if we increase the progression rate of susceptibles into vaccinated and strength of other effective COVID-19 prevention measures, then the transmission of COVID-19 outbreak will end. Figure 9 depicts the physical outlook of the sensitivity analysis when the following values are used: $\phi = 0.063$, $\alpha = 0.82$, $\gamma = 0.51$, and $\psi = 0.999$ while other parameter values are from Table 2 of system of equations (1), which means that parameters with positive indices can cause an outbreak of the COVID-19 pandemic, while parameters with negative indices can slow or stop its spread.

From Figure 10, it is clear that R_0 rises in proportion to the rise in contact rate β and after a certain value of β, R_0 becomes larger than 1. This implies that up to a certain value of R_0, the disease-free equilibrium point is stable and for R_0 greater than 1, the disease-free equilibrium becomes unstable. Figure 11 reveals the variation of R_0 with respect to mitigation measures of the COVID-19 outbreak σ. It can easily be observed that R_0 decreases with an increase in COVID-19 mitigation rate σ and after a certain value of σ, R_0 becomes less than 1. It implies after a certain value of σ, the disease-free equilibrium becomes stable.

Figures 12 and 13 present that the progression rate of the number of susceptible individuals into infectious populations due to COVID-19 infection decreases while the number of the infectious individual class decreases when the values of σ and η increase.

The authors find some significant results which are shown in Figures 14–17 that the number of susceptible and recovered individuals increases with the optimal control and decreases without optimal control, whereas the number of infectious and quarantined individuals decreases with optimal control and increases without optimal control.

The profile of optimal controls u_1 and u_2 is portrayed in Figure 18. From Figure 18, we observe that to control the spread of COVID-19, the use of prevention, u_1, and intervention u_2 strategies must be held effectively.

6. Conclusion and Future Directions

In this study, the authors formulated and analyzed a nonlinear deterministic mathematical model of the COVID-19 outbreak to investigate the impact of vaccination and treatment with optimal control. We have shown the existence and uniqueness, nonnegativity, and invariant region of model solutions under a certain meaningful set. Basic reproduction number R_0 is derived via the help of next-generation approach method, and stability analysis for disease-free equilibrium and endemic equilibrium points is rigorously studied based on this R_0.

It is observed that the disease-free equilibrium is locally as well as globally asymptotically stable whenever the basic reproduction number is less than unity (i.e., COVID-19 dies out in the population). However, the endemic equilibrium point exists and globally asymptotically stable whenever the basic reproduction number is greater than unity (i.e., COVID-19 persists within the society). Sensitivity analysis of the basic reproduction number with respect to model parameters was demonstrated, and it can be inferred that to minimize the COVID-19 outbreak, parameters with positive indices should be decreased while parameters with negative indices should be increased.

The theoretical and numerical studies of the model without control reveal that as the effective mitigations of COVID-19 rates (σ and η) increase, the infected number of individuals decreases in addition to vaccination and treatment. Further, as the contact rate of susceptible and vaccinated individuals with infected individuals decreases, then the number of infected individuals decreases. Then, the model is extended by introducing two time-dependent control variables, educational campaign u_1 and continuous treatment u_2. The qualitative study proved the existence and characterization of an optimal control solution.

The numerical results of the optimal control are illustrated and revealed that the educational campaign u_1 and treatment u_2 control strategies are the most effective strategies in the control of the COVID-19 pandemic. Therefore, authorities and health practitioners have to give great emphasis for the educational campaign to susceptibles and continuous treatment for quarantined individuals in order to eliminate the COVID-19 pandemic. The impact of asymptomatic of COVID-19 human immigrants and cost-effectiveness analysis of the optimal control strategies would be considered in our future study.

Data Availability

The data used to support this study is taken from the previous published papers.

Conflicts of Interest

There is no conflict of interest.

References

[1] H. M. Yang, L. P. L. Junior, F. F. M. Castro, and A. C. Yang, "Mathematical modeling of the transmission of SARS-CoV-2—evaluating the impact of isolation in São Paulo State (Brazil) and lockdown in Spain associated with protective measures on the epidemic of CoViD-19," *PLoS One*, vol. 16, no. 6, article e0252271, 2021.

[2] H. R. Diagne, S. Y. Tchoumi, and J. M. Tchuenche, "A mathematical model of COVID-19 with vaccination and treatment," *Computational and Mathematical Methods in Medicine*, vol. 2021, Article ID 1250129, 16 pages, 2021.

[3] A. A. Anteneh, Y. M. Bazezew, and S. Palanisamy, "Mathematical model and analysis on the impact of awareness campaign and asymptomatic human immigrants in the transmission of COVID-19," *BioMed Research International*, vol. 2022, Article ID 6260262, 13 pages, 2022.

[4] B. Fain and H. M. Dobrovolny, "Initial inoculum and the severity of COVID-19: a mathematical modeling study of the dose-response of SARS-CoV-2 infections," *Epidemiologia*, vol. 1, pp. 5–15, 2020.

[5] N. Zhu, D. Zhang, W. Wang et al., "A novel coronavirus from patients with pneumonia in China, 2019," *The New England Journal of Medicine*, vol. 382, no. 8, pp. 727–733, 2020.

[6] P. Riyapan, S. E. Shuaib, and A. Intarasit, "A mathematical model of COVID-19 pandemic: a case study of Bangkok, Thailand," *Computational and Mathematical Methods in Medicine*, vol. 2021, Article ID 6664483, 11 pages, 2021.

[7] X. P. Li, H. Al Bayatti, A. Din, and A. Zeb, "A vigorous study of fractional order COVID-19 model via ABC derivatives," *Results in Physics*, vol. 29, article 104737, 2021.

[8] L. Zou, F. Ruan, M. Huang et al., "SARS-CoV-2 viral load in upper respiratory specimens of infected patients," *The New England Journal of Medicine*, vol. 382, no. 12, pp. 1177–1179, 2020.

[9] A. Zeb, E. Alzahrani, V. S. Erturk, and G. Zaman, "Mathematical model for coronavirus disease 2019 (COVID-19) containing isolation class," *BioMed Research International*, vol. 2020, Article ID 3452402, 7 pages, 2020.

[10] D. K. Mamo, "Model the transmission dynamics of COVID-19 propagation with public health intervention," *Results in Applied Mathematics*, vol. 7, article 100123, 2020.

[11] N. Chitnis, J. M. Hyman, and J. M. Cushing, "Determining important parameters in the spread of malaria through the sensitivity analysis of a mathematical model," *Bulletin of Mathematical Biology*, vol. 70, no. 5, pp. 1272–1296, 2008.

[12] European Centre for Disease Prevention and Control, *Clinical characteristics of COVID-19*, 2020.

[13] W. J. Guan, Z. Y. Ni, Y. Hu et al., "Clinical characteristics of coronavirus disease 2019 in China," *The New England Journal of Medicine*, vol. 382, no. 18, pp. 1708–1720, 2020.

[14] R. Nigam, K. Pandya, A. J. Luis, R. Sengupta, and M. Kotha, "Positive effects of COVID-19 lockdown on air quality of industrial cities (Ankleshwar and Vapi) of Western India," *Scientific Reports*, vol. 11, no. 1, p. 4285, 2021.

[15] World Health Organization, *Modes of transmission of virus causing COVID19: implications for IPC precaution recommendations: scientific brief*, World Health Organization, 2020.

[16] World Health Organization (WHO), *Coronavirus disease 2019 (COVID-19) situation reports*.

[17] World Health Organization (WHO), *Weekly epidemiological update on COVID-19-5*, 2021.

[18] Z. S. Kifle and L. L. Obsu, "Mathematical modeling for COVID-19 transmission dynamics: a case study in Ethiopia," *Results in Physics*, vol. 34, article 105191, 2022.

[19] K. Hattaf, "A new generalized definition of fractional derivative with nonsingular kernel," *Computation*, vol. 8, no. 2, p. 49, 2020.

[20] I. Holmdahl and C. Buckee, "Wrong but useful—what COVID-19 epidemiologic models can and cannot tell us," *New England Journal of Medicine*, vol. 383, no. 4, pp. 303–305, 2020.

[21] M. Lounis and J. dos Santos Azevedo, "Application of a generalized SEIR model for COVID-19 in Algeria," *European Journal of Sustainable Development Research*, vol. 5, no. 1, article em0150, 2021.

[22] J. Y. T. Mugisha, J. Ssebuliba, J. N. Nakakawa, C. R. Kikawa, and A. Ssematimba, "Mathematical modeling of COVID-19 transmission dynamics in Uganda: implications of complacency and early easing of lockdown," *PLoS One*, vol. 16, no. 2, article e0247456, 2021.

[23] W. M. Sweileh, "Global research activity on mathematical modeling of transmission and control of 23 selected infectious disease outbreak," *Globalization and Health*, vol. 18, no. 1, p. 4, 2022.

[24] I. Ahmed, G. U. Modu, A. Yusuf, P. Kumam, and I. Yusuf, "A mathematical model of coronavirus disease (COVID-19) containing asymptomatic and symptomatic classes," *Results in physics*, vol. 21, article 103776, 2021.

[25] G. T. Tilahun and H. T. Alemneh, "Mathematical modeling and optimal control analysis of COVID-19 in Ethiopia," *Journal of Interdisciplinary Mathematics*, vol. 24, no. 8, pp. 2101–2120, 2021.

[26] S. R. Bandekar and M. Ghosh, "Modeling and analysis of COVID-19 in India with treatment function through different phases of lockdown and unlock," *Stochastic Analysis and Applications*, vol. 40, no. 5, pp. 812–829, 2021.

[27] S. Mwalili, M. Kimathi, V. Ojiambo, D. Gathungu, and R. Mbogo, "SEIR model for COVID-19 dynamics incorporating the environment and social distancing," *BMC Research Notes*, vol. 13, no. 1, p. 352, 2020.

[28] M. A. Khan and A. Atangana, "Mathematical modeling and analysis of COVID-19: a study of new variant omicron," *Physica A*, vol. 599, article 127452, 2022.

[29] X. P. Li, Y. Wang, M. A. Khan, M. Y. Alshahrani, and T. Muhammad, "A dynamical study of SARS-COV-2: a study of third wave," *Results in Physics*, vol. 29, article 104705, 6 pages, 2021.

[30] H. Namawejje, L. S. Luboobi, D. Kuznetsov, and E. Wobudeya, "Modeling optimal control of rotavirus disease with different control strategies," *Journal of Mathematical and Computational Science*, vol. 4, no. 5, p. 892, 2014.

[31] T. T. Ega, M. Y. Dawed, B. K. Gebremeskele, and T. T. Tegegn, "Mathematical model for estimating unconfirmed cases of COVID-19 in-Ethiopia, and targeting sensitive parameters,"

International Journal of Mathematics and Computer Science, vol. 10, pp. 2853–2870, 2020.

[32] A. Shafiq, S. A. Lone, T. N. Sindhu, Y. el Khatib, Q. M. al-Mdallal, and T. Muhammad, "A new modified Kies Frechet distribution: applications of mortality rate of Covid-19," *Results in physics*, vol. 28, article 104638, 2021.

[33] Z. H. Shen, Y. M. Chu, M. A. Khan, S. Muhammad, O. A. Al-Hartomy, and M. Higazy, "Mathematical modeling and optimal control of the COVID-19 dynamics," *Results in Physics*, vol. 31, article 105028, 2021.

[34] K. Dehingia, A. A. Mohsen, S. A. Alharbi, R. D. Alsemiry, and S. Rezapour, "Dynamical behavior of a fractional order model for within-host SARS-CoV-2," *Mathematics*, vol. 10, no. 13, p. 2344, 2022.

[35] I. M. Wangari, S. Sewe, G. Kimathi, M. Wainaina, V. Kitetu, and W. Kaluki, "Mathematical modelling of COVID-19 transmission in Kenya: a model with reinfection transmission mechanism," *Computational and Mathematical Methods in Medicine*, vol. 2021, Article ID 5384481, 18 pages, 2021.

[36] T. N. Sindhu, Z. Hussain, N. Alotaibi, and T. Muhammed, "Estimation method of mixture distribution and modeling of COVID-19 pandemic," *Aims Math*, vol. 7, no. 6, pp. 9926–9956, 2022.

[37] A. Shafiq, A. Batur Colak, T. Naz Sindhu, S. Ahmed Lone, A. Alsubie, and F. Jarad, "Comparative study of artificial neural network versus parametric method in COVID-19 data analysis," *Results in Physics*, vol. 38, article 105613, 2022.

[38] A. S. Bhadauria, R. Pathak, and M. Chaudhary, "A SIQ mathematical model on COVID-19 investigating the lockdown effect," *Infectious Disease Modelling*, vol. 6, pp. 244–257, 2021.

[39] M. Mahrouf, A. Boukhouima, H. Zine, E. M. Lotfi, D. F. M. Torres, and N. Yousfi, "Modeling and forecasting of COVID-19 spreading by delayed stochastic differential equations," *Axioms*, vol. 10, no. 1, p. 18, 2021.

[40] K. G. Mekonen and L. L. Obsu, "Mathematical modeling and analysis for the co-infection of COVID-19 and tuberculosis," *Heliyon*, vol. 8, no. 10, article e11195, 2022.

[41] Q. Liu, D. Jiang, and N. Shi, "Threshold behavior in a stochastic SIQR epidemic model with standard incidence and regime switching," *Applied Mathematics and Computation*, vol. 316, pp. 310–325, 2018.

[42] B. J. Schroers, *Ordinary Differential Equations: A Practical Guide*, Cambridge University Press, 2012.

[43] P. Van den Driessche and J. Watmough, "Further notes on the basic reproduction number," in *Mathematical Epidemiology*, Lecture Notes in Mathematics, F. Brauer, P. Driessche, and J. Wu, Eds., pp. 159–178, 2008.

[44] O. Diekmann, J. A. Heesterbeek, and J. A. Metz, "On the definition and the computation of the basic reproduction ratio R_0 in models for infectious diseases in heterogeneous populations," *Journal of Mathematical Biology*, vol. 28, no. 4, pp. 365–382, 1990.

[45] C. Castillo-Chavez, S. Blower, P. Van den Driessche, D. Kirschner, and A.-A. Yakubu, *Mathematical Approaches for Emerging and Reemerging Infectious Diseases: An Introduction*, Springer Science and Business Media, 2002.

[46] Y. Li and J. S. Muldowney, "On Bendixson′s criterion," *Journal of Difference Equations*, vol. 106, no. 1, p. 39, 1993.

[47] B. Shayak, M. M. Sharma, M. Gaur, and A. K. Mishra, "Impact of reproduction number on multiwave spreading dynamics of COVID-19 with temporary immunity: a mathematical model," *International Journal of Infectious Diseases*, vol. 104, pp. 649–654, 2021.

[48] Y. Marimuthu, B. Nagappa, N. Sharma, S. Basu, and K. K. Chopra, "COVID-19 and tuberculosis: a mathematical model based forecasting in Delhi, India," *Indian Journal of Tuberculosis*, vol. 67, no. 2, pp. 177–181, 2020.

[49] K. Liang, "Mathematical model of infection kinetics and its analysis for COVID-19, SARS and MERS," *Infection, Genetics and Evolution*, vol. 82, article 104306, 2020.

[50] B. Pantha, F. B. Agusto, and I. M. Elmojtaba, "Optimal control applied to a visceral leishmaniasis model," *Electronic Journal of Differential Equations*, vol. 2020, no. 80, pp. 1–24, 2020.

[51] S. Biswas, A. Subramanian, I. M. ELMojtaba, J. Chattopadhyay, and R. R. Sarkar, "Optimal combinations of control strategies and cost-effective analysis for visceral leishmaniasis disease transmission," *PLoS One*, vol. 12, no. 2, article e0172465, 2017.

[52] S. Lenhart and J. T. Workman, *Optimal Control Applied to Biological Models*, Chapman and Hall/CRC, Mathematical and Computational Biology Series, 2007.

[53] E. O. Alzahrani, W. Ahmad, M. Altaf Khan, and S. J. Malebary, "Optimal control strategies of Zika virus model with mutant," *Communications in Nonlinear Science and Numerical Simulation*, vol. 93, article 105532, 2021.

[54] W. E. Boyce and R. C. DiPrima, *Elementary Differential Equations and Boundary Value Problems*, John Wiley and Sons, Inc., 2012.

[55] T. K. Kar and S. Jana, "Application of three controls optimally in a vector-borne disease-a mathematical study," *Communications in Nonlinear Science and Numerical Simulation*, vol. 8, no. 10, pp. 2868–2884, 2013.